Improving the photoresponse spectra of BaSi2 layers by capping with hydrogenated amorphous Si layers prepared by radio-frequency hydrogen plasma

Improving the photoresponse spectra of BaSi$_2$ layers by capping with hydrogenated amorphous Si layers prepared by radio-frequency hydrogen plasma

Zhihao Xu, Kazuhiro Gotoh, Tianguo Deng, Takuma Sato, Ryota Takabe, Kaoru Toko, Noritaka Usami, and Takashi Suemasu

Improving the photoresponse spectra of BaSi₂ layers by capping with hydrogenated amorphous Si layers prepared by radio-frequency hydrogen plasma

Zhihao Xu,[1] Kazuhiro Gotoh,[2] Tianguo Deng,[1] Takuma Sato,[1] Ryota Takabe,[1] Kaoru Toko,[1] Noritaka Usami,[2] and Takashi Suemasu[1,a]

[1]*Institute of Applied Physics, Graduate School of Pure and Applied Sciences, University of Tsukuba, Tsukuba, Ibaraki 305-8573, Japan*
[2]*Graduate School of Engineering, Nagoya University, Nagoya 464-8603, Japan*

We studied the surface passivation effect of hydrogenated amorphous silicon (a-Si:H) layers on BaSi₂ films. a-Si:H was formed by an electron-beam evaporation of Si, and a supply of atomic hydrogen using radio-frequency plasma. Surface passivation effect was first investigated on a conventional n-Si(111) substrate by capping with 20 nm-thick a-Si:H layers, and next on a 0.5 μm-thick BaSi₂ film on Si(111) by molecular beam epitaxy. The internal quantum efficiency distinctly increased by 4 times in a wide wavelength range for sample capped *in situ* with a 3 nm-thick a-Si:H layer compared to those capped with a pure a-Si layer. © *2018 Author(s). All article content, except where otherwise noted, is licensed under a Creative Commons Attribution (CC BY) license (http://creativecommons.org/licenses/by/4.0/).* https://doi.org/10.1063/1.5025021

It is important for solar cell materials to have a large absorption coefficient (α), a suitable band gap, and superior minority-carrier properties to give a high conversion efficiency (η). Semiconducting barium disilicide (BaSi₂),[1,2] composed of earth-abundant elements, has all these properties such as a band gap of 1.3 eV,[3] a large α of 3×10^4 cm⁻¹ at 1.5 eV,[3–6] inactive grain boundaries,[7] and a large minority-carrier lifetime ($\tau \sim 10$ μs).[8,9] Since BaSi₂ can be grown epitaxially on a Si substrate[10] and its band gap can be increased by adding other elements such as Sr and C,[11,12] BaSi₂ is a material of choice for targeting $\eta > 30\%$ in Si-based tandem structure solar cells. We have achieved η approaching 10% in a p-BaSi₂/n-Si heterojunction solar cell capped with a pure amorphous Si (a-Si) layer by an electron-beam (EB) evaporation.[13,14] The a-Si capping layer prevents oxidation of the BaSi₂ surface and acts as a good electrical contact for hole transport in the a-Si/BaSi₂ structure, which was evidenced by hard x-ray photoelectron spectroscopy.[15] Surface passivation is very important for materials like BaSi₂, which possess large α, because the short-wavelength light is absorbed in the region close to the surface. For example, α reaches 5×10^5 cm⁻¹ at a wavelength of 400 nm for BaSi₂,[5] meaning that most of the photons at this wavelength are absorbed as they pass only 60 nm ($1/\alpha \times 3 = 60$ nm) through the BaSi₂ layer, and electrons and holes are generated. Therefore, defective surface deteriorates the solar cell performance. According to surface structure analysis of BaSi₂ epitaxial layers using Coaxial-Collision Ion Scattering Spectroscopy by Katayama *et al.*,[16,17] an *a*-axis-oriented BaSi₂ epitaxial film is terminated by Si₄ tetrahedra. First-principle calculations revealed that Si vacancies in Si₄ tetrahedra are most likely to exist as native point defects in BaSi₂,[18] and induce localized states within the band gap. Actually, the photoresponsivity, carrier type, and carrier concentration of undoped 0.5 μm-thick BaSi₂ epitaxial films are quite sensitive to Si vacancies.[19] Therefore, the capping of a BaSi₂ layer with a hydrogenated a-Si (a-Si:H) layer rather than a pure a-Si layer is considered preferable for BaSi₂ from the viewpoint of surface passivation of topmost Si₄ tetrahedra. However, there has been no report on how effective an a-Si:H capping layer behaves on BaSi₂. By using a-Si:H to passivate crystalline Si (c-Si) surface, the outstanding carrier lifetime and surface recombination velocity were obtained.[20] The most common method to form a-Si:H layers is plasma-enhanced chemical vapor

---

[a]Corresponding author: suemasu@bk.tsukuba.ac.jp

deposition (PECVD),[21] where silane is decomposed by radio frequency (RF) plasma. In this paper, we form a-Si:H layers by an easier method than PECVD, that is an EB evaporation of Si with a simultaneous supply or a subsequent supply of atomic hydrogen using RF plasma. Internal quantum efficiencies (*IQE*) of BaSi$_2$ films capped with a-Si:H layers were drastically improved by a factor of 4 compared to those capped with pure a-Si layers.

An ion-pumped molecular beam epitaxy (MBE) system equipped with a standard Knudsen cell for Ba, an EB gun for Si, and an RF plasma source for atomic hydrogen was used in this experiment. The details of all samples are summarized in Table I. Regarding the substrate temperature (T_S) during the deposition of a-Si, a-Si:H depositions at $T_S = 180-200\,°C$ are recommended in PECVD.[22] Besides, even a pure a-Si capping layer deposited at $T_S = 180\,°C$ acts as a passivation layer for BaSi$_2$.[13,14] We hence set T_S at $180\,°C$ in many samples.

Firstly, we formed approximately 150 nm-thick a-Si:H layers on Al(200 nm)-covered n-Si substrate to confirm the presence of Si-H bonds in the grown layers (sample B−G). The Al layer eliminates the Raman signals related to the Si substrate. We set the RF power at 70 W and the vacuum level at 10^{-3} Pa for atomic hydrogen, and applied two different growth methods, that is the post-deposition (PD) method and the co-deposition (CD) method. The difference between these two methods is whether the hydrogen plasma was supplied to the a-Si layer subsequently or simultaneously. T_S and hydrogen supply duration (t_H) were the parameters to be controlled. For comparison, we deposited a pure a-Si layer at $T_S = 180\,°C$ on Al/c-Si (sample A). Raman spectra were measured by Raman spectrometer (JASCO, NRS-5100) using a frequency doubled Nd: YAG laser (532 nm, 5.1 mW). The spectral resolution was not worse than 4.2 cm^{-1}. Secondly, we confirmed the passivation effect of approximately 20 nm-thick a-Si:H layers in samples H and I by measuring the effective carrier lifetime (τ) of a medium-doped Czochralski (CZ) n-type Si(111) substrate (resistivity $\rho = 6-9\,\Omega cm$) using a quasi-steady-state photoconductivity method (QSSPC; Sinton Instruments, WCT-120 lifetime tester). For this purpose, we mirror-polished both front and back surfaces of the Si(111) substrate, and deposited a-Si:H layers on both sides at $180\,°C$. Thirdly, we applied a-Si:H layers to approximately 0.5 μm-thick undoped-BaSi$_2$ epitaxial films on a low-ρ CZ n$^+$-Si(111) substrate ($\rho < 0.009\,\Omega cm$) for photoresponse measurement. Such a low-ρ substrate makes the contribution of photogenerated carriers in the Si substrate negligible. After the MBE growth, 3 nm-thick a-Si or a-Si:H capping layers were deposited at $180\,°C$ for sample K−N. Then, 80 nm-thick indium-tin-oxide (ITO) electrodes with a diameter of 1 mm were sputtered on the front side and 150 nm-thick Al was sputtered at the back side. Photoresponse spectra were evaluated by a lock-in technique using a xenon lamp with a 25-cm-focal-length single monochromator (Bunko Keiki, SM- 1700A and RU-60N). The light intensity of the lamp was calibrated using a pyroelectric sensor (Melles Griot, 13PEM001/J). Reflectance spectra were evaluated with a reflection measurement system using a xenon lamp with an integrating sphere. The depth profile of H atoms was characterized by secondary ion mass spectrometry (SIMS) by using 3.0 kV Cs$^+$ primary ions. All measurements were performed at room temperature.

TABLE I. Sample preparation details: structure, a-Si thickness (d_{a-Si}), fabrication method, substrate temperature (T_S), hydrogen irradiation duration (t_H), a-Si deposition duration (t_{Si}), and peak position of Si$_{TO}$ are specified.

| Sample	Structure	d_{a-Si} (nm)	Method	T_S (°C)	t_H (min)/t_{Si} (min)	Si$_{TO}$ (cm^{-1})
A	a-Si/Al/c-Si	150	Deposition	180	0/180	468.2
B	a-Si:H/Al/c-Si	150	CD	180	180/180	470.2
C	a-Si:H/Al/c-Si	150	PD	180	60/180	470.9
D	a-Si:H/Al/c-Si	150	PD	180	90/180	470.9
E	a-Si:H/Al/c-Si	150	PD	180	180/180	471.8
F	a-Si:H/Al/c-Si	150	CD	280	180/180	471.9
G	a-Si:H/Al/c-Si	150	CD	80	180/180	501.3
H	a-Si/c-Si/a-Si	20	Deposition	180	0/20	
I	a-Si:H/c-Si/a-Si:H	20	PD	180	10/20	
K	a-Si/BaSi$_2$/Si	3	Deposition	180	0/3.5	
L	a-Si:H/BaSi$_2$/Si	3	PD	180	1.75/3.5	
M	a-Si:H/BaSi$_2$/Si	3	PD	180	5/3.5	
N	a-Si:H/BaSi$_2$/Si	3	CD	180	3.5/3.5	
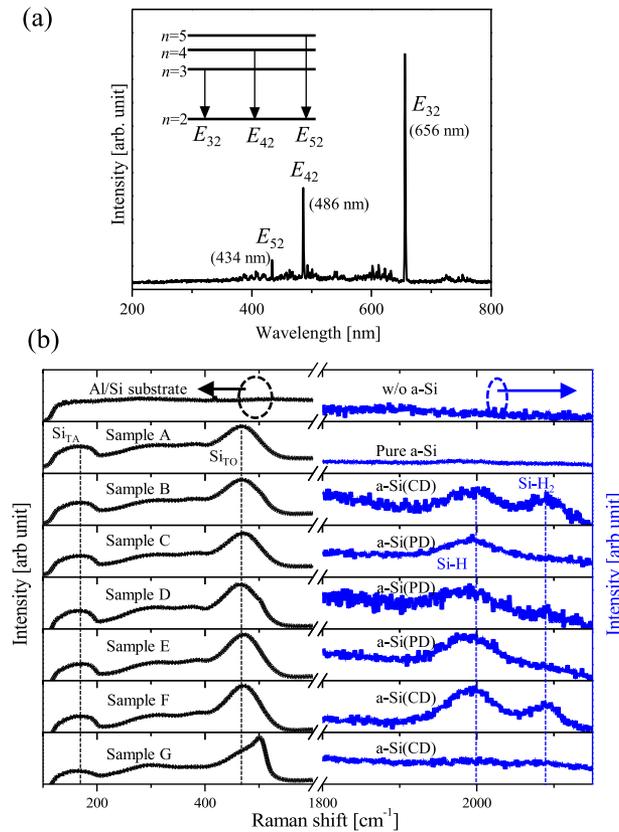
FIG. 1. (a) Representative emission spectrum of hydrogen plasma set at 70 W and 10^{-3} Pa. (b) Raman spectra of Al(200 nm)/c-Si sample and approximately 150 nm-thick a-Si and a-Si:H layers formed on Al(200 nm)/c-Si in samples A−G.

Figure 1(a) shows a representative emission spectrum of hydrogen plasma obtained at 70 W. In the hydrogen plasma spectrum, three peaks denoted by E_{32}, E_{42}, and E_{52} correspond to electron transitions from excited states (n=3, 4, and 5) to the first excited state (n=2), respectively, belonging to the Balmer series.[23] The Raman spectra of samples A−G are shown in Fig. 1(b). Raman peaks due to Si-Si bonds in a-Si such as transverse acoustic (TA) phonon and transverse optical (TO) phonon can be seen at around 180 and 480 cm^{-1},[24] respectively, in all the samples except the Al/Si sample. No evidence of the peak at 520 cm^{-1} indicating scattering from TO-like phonons in crystalline Si was observed. These Raman scattering results confirm that thin films are a-Si layers. Table I summaries the peak position at around 480 cm^{-1} in samples A-G. The nanocrystalline volume fraction of a-Si increases upon hydrogen exposure,[25] leading to the peak shift to higher wavenumbers. S. Sriraman *et al.* investigated hydrogen-induced crystallization of a-Si upon exposure to hydrogen through a combination of molecular-dynamics simulations and *in situ* attenuated total-reflection Fourier-transform infrared spectroscopy.[26] They found that hydrogen atoms rearrange the a-Si network to crystallize even at very low temperatures. This is in contrast to thermal annealing, which leads to crystallization as a result of thermal fluctuations at high temperatures. In samples B−F, Raman peaks corresponding to vibrations of Si-H bonds were observed at around 2000 cm^{-1},[27] meaning that Si-H bonds were formed by the irradiation of hydrogen by both the CD and PD methods. Raman peaks due to the vibrations due to Si-H_2 bonds were observed at 2090 cm^{-1} in samples B and F. In contrast, the formation of Si-H_2 bonds was not detected in samples C−E formed by the PD method regardless of t_H. These results imply that the Si-H_2 bonds were formed only by the CD method. In sample G, however, both Si-H and Si-H_2 bonds did not exist, meaning that T_S = 80 °C is not sufficient to form Si-H bonds. It was reported by Nakamura *et al.*,[28] that the Si-H_2 bonds are responsible for light-induced degradation of a-Si solar cells. On the basis of these results, we chose the PD method rather than the CD method and went forward to the next experiment. Figure 2 shows the SIMS depth profile of hydrogen and secondary ions (Si, Al) intensities
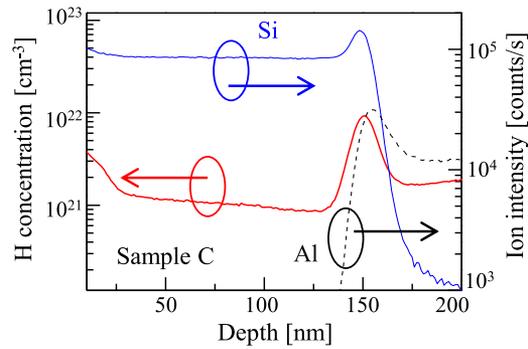
FIG. 2. SIMS depth profile of hydrogen atoms and secondary ions (Si, Al) in sample C.

in sample C, formed by the PD method. The hydrogen concentration was found to be approximately 1×10^{21} cm^{-3} in the a-Si:H layer. Please note that the hydrogen concentration was corrected only in the a-Si layer in Fig. 2 using a reference sample, where controlled number of hydrogen atoms was doped.

The values of τ of samples H and I were measured by QSSPC and compared with that of the same Si substrate without a-Si capping layers in Fig. 3. The density of photoexcited electron-hole pairs was approximately 1×10^{15} cm^{-3}. The τ increased distinctly from approximately 8 μs for the bare Si substrate to 12 μs for sample H, capped with pure a-Si layers, and further to 17 μs for sample I, capped with a-Si:H layers, demonstrating that the capping with a a-Si:H layer formed by the PD method is an effective means to passivate the defective surface states of the c-Si substrate. It should be noted that these measured values of τ were smaller than those reported for conventional c-Si with a similar ρ. Among many factors which affect recombination losses, we suppose that the surface recombination is dominant because we ourselves mirror-polished the back surfaces of the Si(111) substrate used.

Next, we discuss the photoresponse spectra of samples K−N as shown in Fig. 4(a). The bias voltage of −0.3 V was applied to the ITO electrode with respect to the Al electrode so that the photogenerated holes would be extracted to the ITO electrode. The measured photoresponsivities were converted into *IQE* values using the reflectance spectra. The *IQE* began to increase sharply for wavelengths λ shorter than approximately 1000 nm, which corresponds to the band gap of BaSi$_2$. The *IQE* was the smallest for sample K, BaSi$_2$ capped with a pure a-Si layer, and was improved by capping with a a-Si:H layer formed by the CD method in sample N. Much further improvement was achieved for samples L and M, BaSi$_2$ capped with a-Si:H layers by the PD method. We note here that the *IQE* was higher for sample M (t_H = 5 min) than sample L (t_H = 1.75 min). These results provide
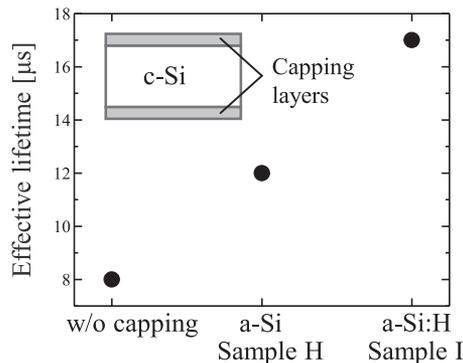

FIG. 3. Effective carrier lifetimes of c-Si(111) substrate (ρ = 6−9 Ωcm), and the c-Si(111) substrates covered on both front and back mirror surfaces with approximately 20 nm-thick pure a-Si (sample H) and a-Si:H layers (sample I). The density of photoexcited electron and hole pairs was approximately 10^{15} cm^{-3}.
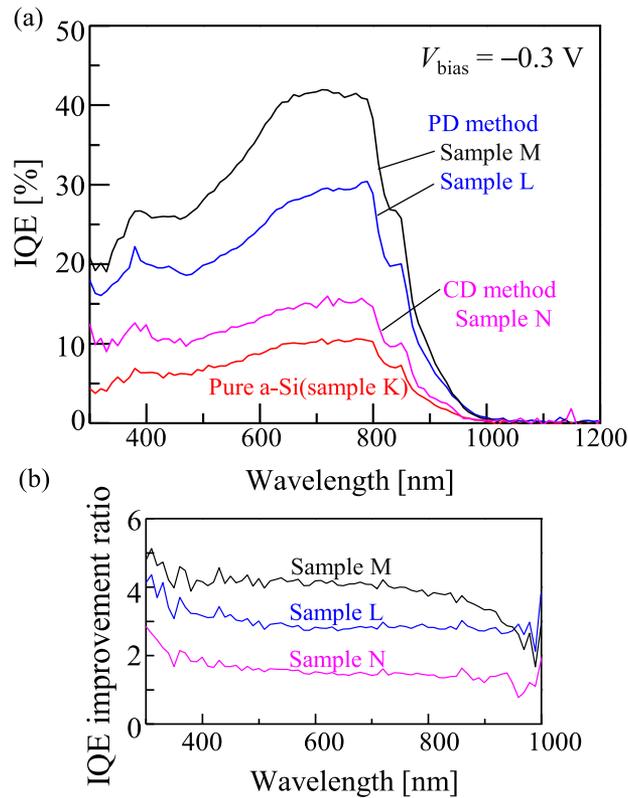
FIG. 4. (a) *IQE* spectra of approximately 0.5 μm-thick BaSi$_2$ layers capped with approximately 3 nm-thick pure a-Si (sample K) and a-Si:H layers (samples L−N). The bias voltage of −0.3 V was applied to the front ITO electrode with respect to the n-Si substrate. (b) *IQE* improvement ratio of samples L−N normalized using those of sample K.

strong evidence that a-Si:H is more preferable than pure a-Si for BaSi$_2$. As for the CD method, we speculate that the hydrogen atoms stroke the BaSi$_2$ surface at the initial formation stage of the a-Si:H layer and hence the *IQE* was suppressed in sample N compared to those of samples M and L formed by the PD method.

Figure 4(b) shows the *IQE* improvement ratio of samples L−N normalized using that of sample K. The *IQE* values of sample M were larger by a factor of 4 than those of sample K. The *IQE* improvement was pronounced especially in the short wavelength region ($\lambda < 400$ nm). This is interpreted to originate from reduced interface states at the a-Si:H/BaSi$_2$, suppressing the recombination of photogenerated carriers in the region close to the surface. The *IQE* was improved over the wide λ range in contrast to our prediction. We suppose that the diffused hydrogen atoms might passivate the defect levels in the bulk region of BaSi$_2$, leading to the improvement of *IQE* spectra in a wide wavelength range.

In summary, we have formed a-Si:H layers by an EB evaporation of Si and a supply of atomic hydrogen using RF plasma. The Si-H bonds were confirmed by Raman spectroscopy and the density of hydrogen atoms was approximately 10^{21} cm^{-3} by SIMS. a-Si:H layers formed by the CD method contained both Si-H and Si-H$_2$ bonds, whereas those by the PD method did not contain Si-H$_2$ bonds. That's why we chose the PD method. Surface passivation effect of a-Si:H layers formed by the PD method at 180 °C was confirmed by the increase of the τ of c-Si ($\rho = 6-9$ Ωcm) capped with a-Si:H layers. It was increased from approximately 8 for the bare c-Si substrate to 17 μs by QSSPC. The *IQE* of a 0.5 μm-thick BaSi$_2$ film capped *in situ* with a 3 nm-thick a-Si:H layer by the PD method at 180 °C was improved by a factor of 4 compared to those capped with a pure a-Si capping layer especially in the short wavelength region $\lambda < 400$ nm. Thereby, the capping of a BaSi$_2$ film with a a-Si:H layer is a very effective means to improve the photoresponsivity of BaSi$_2$. This is an important achievement for solar cell applications of BaSi$_2$.

[1] J. Evers, G. Oeh-ger, and A. Weiss, Angew. Chem. Int. Ed. Engl. **16**, 659 (1977).

[2] M. Imai and T. Hirano, J. Alloys. Compd. **224**, 111 (1995).

[3] K. Morita, Y. Inomata, and T. Suemasu, Thin Solid Films **508**, 363 (2006).

[4] D. B. Migas, V. L. Shaposhnikov, and V. E. Borisenko, Phys. Status Solidi (b) **244**, 2611 (2007).

[5] K. Toh, T. Saito, and T. Suemasu, Jpn. J. Appl. Phys. **50**, 068001 (2011).

[6] M. Kumar, N. Umezawa, and M. Imai, Appl. Phys. Express **7**, 071203 (2014).

[7] M. Baba, M. Kohyama, and T. Suemasu, J. Appl. Phys. **120**, 085311 (2016).

[8] K. O. Hara, N. Usami, K. Toh, M. Baba, K. Toko, and T. Suemasu, J. Appl. Phys. **112**, 083108 (2012).

[9] K. O. Hara, N. Usami, K. Nakamura, R. Takabe, M. Baba, K. Toko, and T. Suemasu, Appl. Phys. Express **6**, 112302 (2013).

[10] R. A. McKee and F. J. Walker, Appl. Phys. Lett. **63**, 2818 (1993).

[11] K. Morita, M. Kobayashi, and T. Suemasu, Jpn. J. Appl. Phys. **45**, L390 (2006).

[12] Y. Imai and A. Watanabe, Intermetallics **18**, 1432 (2010).

[13] D. Tsukahara, S. Yachi, H. Takeuchi, R. Takabe, W. Du, M. Baba, Y. Li, K. Toko, N. Usami, and T. Suemasu, Appl. Phys. Lett. **108**, 152101 (2016).

[14] S. Yachi, R. Takabe, H. Takeuchi, K. Toko, and T. Suemasu, Appl. Phys. Lett. **109**, 072103 (2016).

[15] R. Takabe, H. Takeuchi, W. Du, K. Ito, K. Toko, S. Ueda, A. Kimura, and T. Suemasu, J. Appl. Phys. **119**, 165304 (2016).

[16] S. Okasaka, O. Kubo, D. Tamba, T. Ohashi, H. Tabata, and M. Katayama, Surf. Sci. **635**, 115 (2015).

[17] O. Kubo, T. Otsuka, S. Okasaka, S. Osaka, H. Tabata, and M. Katayama, Jpn. J. Appl. Phys. **55**, 08NB11 (2016).

[18] M. Kumar, N. Umezawa, W. Zou, and M. Imai, J. Mater. Chem. A **5**, 25293 (2017).

[19] R. Takabe, T. Deng, K. Kodama, Y. Yamashita, T. Sato, K. Toko, and T. Suemasu, J. Appl. Phys. **123**, 045703 (2018).

[20] J.-W. A. Schüttauf, K. H. M. van der Werf, I. M. Kielen, W. G. J. H. M. van Sark, J. K. Rath, and R. E. I. Schropp, Appl. Phys. Lett. **98**, 153514 (2011).

[21] R. C. Chittick, J. H. Alexander, and H. F. Sterling, J. Electrochem. Soc. **116**, 77 (1969).

[22] J. Müllerová, M. Fischer, M. Netrvalová, M. Zeman, and P. Šutta, Cent. Eur. J. Phys. **9**, 1301 (2011).

[23] P. J. Mohr, B. N. Taylor, and D. B. Newell, Rev. Mod. Phys. **84**, 1527 (2012).

[24] V. A. Volodin and D. I. Koshelev, J. Raman. Spectrosc. **44**, 1760 (2013).

[25] A. McEvoy, T. Markvart, and L. Castaner, *Practical Handbook of Photovoltaics*, Part IC-1 (Academic Press, New York, 2012), 2nd ed.

[26] S. Sriraman, S. Agarwal, E. S. Aydil, and D. Maroudas, Nature **418**, 62 (2002).

[27] D. A. Strubbe, E. C. Johlin, T. R. Kirkpatrick, T. Buonassisi, and J. C. Grossman, Phys. Rev. B **92** (2015).

[28] N. Nakamura, T. Takahama, M. Isomura, M. Nishikuni, K. Yoshida, S. Tsuda, S. Nakano, M. Ohnishi, and Y. Kuwano, Jpn. J. Appl. Phys. **28**, 1762 (1989).